Bioscience Reports (2020) **40** BSR20191571
https://doi.org/10.1042/BSR20191571

PORTLAND PRESS

Research Article

Long non-coding RNA PSMA3-AS1 enhances cell proliferation, migration and invasion by regulating miR-302a-3p/RAB22A in glioma

Li-li Zhou[1], Meng Zhang[2], Yan-zhen Zhang[1] and Mei-fen Sun[1]

[1]Department of Neurology, Heze No. 3 People's Hospital, Heze, Shandong, China; [2]Health Management Center, Zaozhuang Traditional Chinese Medicine Hospital, Zaozhuang, Shandong, China

Correspondence: Mei-fen Sun (sdsunmeifen@163.com)

Glioma is the most prevalent solid tumor in the central nervous system (CNS). Recently, it has been indicated that long non-coding RNAs (lncRNAs) substantially adjust the development of a variety of human cancers. In the present study, it was found and verified via microarray analysis that lncRNA *PSMA3-AS1* exhibited a high expression in glioma tissues and cell lines. Then CCK-8, 5-Ethynyl-2′-deoxyuridine (EdU) staining, plate clone assay, Transwell assay, Western blotting and nude mouse model were adopted to verify *PSMA3-AS1*'s effects on glioma. Knockdown of *PSMA3-AS1* inhibited the migration, proliferation and invasion of glioma cells *in vivo* and *in vitro*. Besides, *PSMA3-AS1* bound to miR-302a-3p directly reduced the expression of miR-302a-3p, thus functioning as an endogenous sponge confirmed by luciferase reporter assay and bioinformatics analysis. *PSMA3-AS1* knockdown remarkably enhanced the role of miR-302a-3p overexpression in cell behaviors in glioma. Moreover, these assays also confirmed that *RAB22A* was a target of miR-302a-3p. In this research, therefore, the *PSMA3-AS1*/miR-302a-3p/*RAB22A* pathway regulatory axis may be revealed in the pathogenesis of glioma, and *PSMA3-AS1* can be used as an underlying target for the treatment and prognosis of glioma.

Introduction

As the most common solid tumor, glioma is the most common solid tumor in the central nervous system (CNS) [1,2]. Glioma in the CNS has been classified into the low and high grade by the World Health Organization (WHO), based on which low-grade glioma is further subdivided into Grades I and II, while high-grade glioma into Grades III and IV [3]. Generally, cases of Grade IV glioma (glioblastomas; GBMs) die within 2 years, and cases of Grade III anaplastic glioma and Grade II glioma have 2–5- and 2-year prognosis, respectively [4]. Hence, investigating the potential molecular mechanisms of glioma development and progression should be the top priority for enhancing the diagnosis and treatment of the tumor.

Long non-coding RNAs (lncRNAs) are a type of RNAs with length over 200 nucleotides that have no coding ability [5]. Besides, multiple biological processes, including cell apoptosis, proliferation and metastasis in cancers are modulated by lncRNAs [6–8]. There are many lncRNAs related to glioma that have been reported. For example, Xia et al. confirmed that *FER1L4* adjusts the cycle and proliferation of glioma cells [9], Ni et al. proposed that *FoxD2-AS1* adjusts the PI3K/AKT signaling pathway as well as the miR-185-5P/*HMGA2* axis, so as to accelerate the progression of glioma [10], and Yang et al. found that lncRNA *HERC2P2* is a tumor suppressor in glioma [11]. However, there are still many gaps in our current understanding of lncRNA function. *PSMA3-AS1* (ENSG00000257621) is an lncRNA located on chromosome 14q23.1, and no reports examine the role of *PSMA3-AS1* in glioma.

Received: 04 June 2019
Revised: 23 April 2020
Accepted: 20 May 2020

Accepted Manuscript online: 07 September 2020
Version of Record published: 21 September 2020

Bioscience Reports (2020) **40** BSR20191571
https://doi.org/10.1042/BSR20191571

Table 1 Clinical information of glioma patients

Parameters	Group	Cases	PSMA3-AS1 expression				*P*-value
			Low	%	High	%	
Gender	Male	13	7	53.8	6	46.2	0.819
	Female	7	4	57.1	3	42.9	
Age at surgery (years)	<30	6	4	66.7	2	33.3	0.755
	>30	14	7	50	7	50	
Pathological stage	WTO: I–II	5	5	100	0	0	0.035
	WTO: III–IV	15	6	40	9	60	
Tumor size (maximum diameter in MRI)	≥ 30 mm	10	6	60	4	40	0.613
	<30 mm	10	5	50	5	50	
Tumor necrosis	Yes	7	3	42.9	4	57.1	0.256
	No	13	8	61.5	5	38.5	
Total		20	10	50	10	50	

In recent years, it has been widely investigated that lncRNAs interact with miRNAs, becoming a mechanism associated with the tumor biology mediated by lncRNAs. MiRNAs are relatively conservative with 18–22 nt in length, which are different from lncRNAs [12]. MiRNAs boost the degradation of RNAs in mammals and bind to the 3′-untranslated region (3′UTR) of target mRNAs, thus modulating negative genes [13]. Different biological processes contained and are controlled by a variety of miRNAs. By reference to the definition of competing endogenous RNAs (ceRNAs), RNAs compete for shared miRNAs to interact with each other, which implies another method of post-transcriptional regulation [14]. Then, the miR-302a-3p was selected based on the StarBase database through bioinformatics prediction. Moreover, miR-302a-3p dampens the initiation and development of cancers, such as pancreatic cancer and hepatocellular carcinoma by interaction with various downstream targets [15,16]. However, the potential mechanism in which miR-302a-3p functions is still rarely reported.

As such, it was speculated that *PSMA3-AS1* contributed to malignant glioma behaviors by adjusting miR-302a-3p/*RAB22A*. To validate this, the expression pattern of *PSMA3-AS1* in glioma tissues and cell lines was first studied, followed by investigation of its biological effects and clinical value in glioma. Ultimately, the *PSMA3-AS1*/miR-302a-3p/*RAB22A* pathway was validated to be related to the growth, invasion and migration of glioma, so it was considered as an underlying target in the diagnosis and treatment of glioma.

Materials and methods

Clinical tissue samples

Twenty pairs of glioma tissue and adjacent normal tissue samples were extracted from cases who underwent routine surgery with glioma confirmed by pathology in Heze No. 3 People's Hospital from January 2017 to December 2018. All the cases underwent no radiotherapy or chemotherapy prior to surgery, and they signed the informed consent. Immediately after extraction, all tissue samples were frozen in liquid nitrogen for later assays. Detailed information is presented in Table 1. This research was approved by the Ethics Committee of Heze No. 3 People's Hospital.

Cell lines and cell culture

A172, LN229, U87 and U251, glioma cell lines, and NHA, a human normal astrocyte cell line, were provided by the Cell Bank of CAS (Shanghai, China), purchased from Thermo Fisher Scientific and maintained in DMEM (Gigliomao, Carlsbad, CA, U.S.A.) supplemented with 10% FBS (Gigliomao) under the conditions of 5% CO_2 at 37°C.

Quantitative real-time PCR

TRIzol (Life Technologies, Carlsbad, U.S.A.) was utilized to separate total RNAs from tissues and cells, and RNAs were synthesized into cDNAs using PrimeScript RT Reagent Kit, or into miRNAs using the PrimeScript miRNA cDNA Synthesis Kit (TaKaRa, Tokyo, Japan) by reference to the manufacturer's schemes. SYBR® Premix ExTaq™ reagent (TaKaRa) was used for qPCR on the ABI PRISM 7500 RT-PCR system (Applied Biosystems, Foster City, CA, U.S.A.). Gene expression was monitored with GADPH or U6 expression as an internal reference. Designed by RiboBio

(Guangzhou, China), primer sequences are shown below: *PSMA3-AS1*: F: 5′-GUCGGUCAGGUUGGUGUCUA-3′ and R: 5′-GCUGUGAAAGUGCCUGUGAA-3′; miR-302a-3p: F: 5′-ACACUCCAGCUGGGAGUGGUUUUGUACCUUC-3′ and R: 5′-CUCAACUGGUGUCGUGGAGUCGGCAAUUCAGUUGAGUCGUGAAU-3′; *RAB22A*: F: 5′-GUGUGUCUGCUCGGGGAUAC-3′ and R: 5′-GCCCCUAUUGUUGGGUUGAUGU-3′; GAPDH: F: 5′-GTCAACGGATTTGGTCTGTATT-3′ and R: 5′-AGTCTTCTGGGTGGCAGTGAT-3′; U6: F: 5′-CTCGCTTCGGCAGCACA-3′ and R: 5′-AACGCTTCACGAATTTGCGT-3′. $2^{-\Delta\Delta C_t}$ method was adopted to calculate the relative expression level.

Subcellular fractionation

The nuclear and cytosolic fractions of LN229 and U251 cells were separated using the PARIS Kit (Invitrogen, U.S.A.) according to the manufacturer's instructions. RNA was extracted from both fractions. Quantitative real-time PCR (qRT-PCR) was then performed using GAPDH as the cytosolic control, and U6 as the nuclear control.

Cell transfection

Small interfering RNAs (siRNAs) specifically targeting *PSMA3-AS1*, negative control siRNA (si-NC), miR-302a-3p mimics and miR-NC were provided by Shanghai GenePharma Co., Ltd. (Shanghai, China). The sequence of PSMA3-AS1 siRNA, miR-302a-3p mimics and miR-NC are as below: si-PSMA3-AS1-1: 5′- UCUCGAAAACCCGAAAGAGAA-3′; si-PSMA3-AS1-2: 5′-UUCUAAGAACCACUUCUUCCC-3′; miR-NC: 5′-UCACAACCUCCUAGAAAGAGUAGA-3′; miR-302a-3p mimics: 5′-UAAGUGCUUCCAUGUUUUGGUGA-3′; miR-302a-3p inhibitor: 5′-UAAGUGCUUCCAUGUUUUGGUGA-3′. By reference to the manufacturer's protocol, Lipofectamine 2000 kit (Invitrogen, CA, U.S.A.) was used to transfect LN229 and U251.

CCK-8 assay

Transfected glioma cells were cultured for 48 h and collected in the logarithmic phase. The cells were generated and seeded in 96-well plates at a density of 5000 cells per well and cells were cultured at 37°C for 24 h. Then 10 μl CCK-8 solution (Solarbio, Beijing, China) was added into each well for 2 h and the absorbance (450 nm) was measured by means of a microplate reader (BioTek Instruments, U.S.A.). Finally, the cell growth curve was plotted in accordance with the absorbance at each time point.

5-Ethynyl-2′-deoxyuridine (EdU) staining

Cell-Light EdU DNA Cell Proliferation Kit (RiboBio Co., Ltd, Guangzhou, China) was applied to assess cell proliferation based on the manufacturer's scheme. Specifically, cells were inoculated in 96-well plates at a density of 5000 cells/well after transfection, and each well was in triplicate. Following culture for 12 h, 4% formaldehyde was added to fix the cells and 100 μl of 1× Apollo® reaction buffer for 30 min of cell incubation. After that, Hoechst 33342 was utilized to stain the cell nuclei for 30 min. The images of cells stained with 5-Ethynyl-2′-deoxyuridine (EdU) and Hoechst were observed under an optical microscope (Nikon, Tokyo, Japan), and EdU-positive cells were counted using ImageJ software.

Colony formation assays

In the first place, cell cultures were trypsinized to prepare single-cell suspensions, followed by inoculation into six-well plates at 150 cells/well and incubation at 37°C for 14 days. Following formation, methanol was added to fix visible colonies and 0.5% Crystal Violet was used to stain them, followed by cell count in each colony. Colonies formed with over 50 cells were calculated and recorded for statistical analysis.

Cell migration and invasion assays

The 24-well Transwell chamber with polycarbonate membrane (pore size: 8 μm) (EMD Millipore, Billerica, MA, U.S.A.) was utilized to evaluate the invasion and migration abilities of glioma cells *in vitro*. In invasion assay, the cells were added with trypsin after transfection and with medium for suspension, and 20 μl Matrigel (BD Biosciences, San Jose, CA, U.S.A.) was used to pre-coat the upper surface of the filter. In migration assay, the cells received the same treatment as the invasion assay except that the upper chamber was added with 2×10^4 cells in medium free of serum, while the lower chamber was added with medium containing 10% FBS. Subsequently, the cells were incubated for 24 h, after which those that migrated to the lower chamber were subjected to fixation by 4% paraformaldehyde and dying with 0.05% Crystal Violet. At least three fields of view were selected, in which the stained cells were photographed and calculated.

Bioscience Reports (2020) **40** BSR20191571
https://doi.org/10.1042/BSR20191571

Western blotting

RIPA lysis buffer (Beyotime, Beijing, China) was applied for extraction of the total proteins and the Bradford method for protein quantification. SDS/PAGE (10% gel) was carried out to isolate 30 μg protein lysates, and the proteins were then transferred to PVDF membranes (Millipore, Billerica, MA, U.S.A.). Thereafter, these membranes were sealed with 5% skim milk for 1.5 h, followed by incubation with the following primary antibodies: rabbit anti-human *IgG* antibodies and antibodies against *Vimentin* (1:500, ab45939), β-*actin* (1:500, ab8227), *Snail 1* (1:500, ab82846), *ZO-1* (1:500, ab96587), *TSG101* (1:1000, ab125011), *E-cadherin* (1:500, ab11512) and *Twist* (1:500, ab50581) (Agliomaam, Cambridge, MA, U.S.A.). Data analysis was conducted using ImageJ software (NIH, Washington, DC, U.S.A.), and each assay was repeated for three times, respectively.

Luciferase activity assay

Some DNA sequences of *PSMA3-AS1* and *RAB22A* 3′UTRs containing the binding sites for wildtype (WT) or mutant (MUT) miR-302a-3p were subjected to PCR amplification and cloned into pmirGLO luciferase vectors (Promega, Madison, U.S.A.) to produce *RAB220A* WT, *RAB22A* MUT, *PSMA3-AS1* WT and *PSMA3-AS1* MUT reporter plasmids, respectively, so as to elucidate whether *PSMA3-AS1* and *RAB22A* 3′UTRs were directly targeted by miR-302a-3p. During the luciferase assay, the constructed reporter plasmids and miR-302a-3p or miR-NC were applied to independently co-transfect 293T cells by means of Lipofectamine 2000 (Invitrogen, CA, U.S.A.), and the Dual-Luciferase® Reporter Assay kit (Promega) was utilized to examine the luciferase activity at 48 h after transfection based on the manufacturer's scheme.

Tumor formation experiment in nude mice

Nude mice at the age of 6 weeks were bought from Cancer Institute of the Chinese Academy of Medical Science. Both sides of the flank area of mice (n=3) in each group were injected with approximately 1×10^6 U251 that were stably transfected by sh-NC, sh-*PSMA3-AS1* or sh-*PSMA3-AS1*+miR-302a-3p inhibitor lentivirus in 0.1 ml PBS. The tumor volume was calculated using a caliper from the seventh day by reference to the formula $V = (L \times W^2)/2$ (L, length; W, width of the tumor) every 3 days. Based on the average tumor volume, the growth curve was drawn in each group. Thirty-one days later, mice were intraperitoneally injected with 3% pentobarbital sodium and were killed by excessive anesthesia at a dose of 90 ml/kg, and the tumors were removed for follow-up study. Animal experiments took place in SPF Animal Laboratory at Taishan Medical University. Subsequently, qRT-PCR was carried out to detect the expression of *RAB22A* or miR-302a-3p. All assays obtained the approval from the Animal Care and Use committee of the Heze No. 3 People's Hospital and Taishan Medical University with the approval number of 201710012-1. And all *in vivo* experiments were performed in Taishan Medical University.

Statistical analysis

SPSS 22.0 (IBM, SPSS, Chicago, IL, U.S.A.) was adopted for statistical processing. The paired-samples t test was conducted to assess the differences in the expression between glioma tissues and paired adjacent normal tissues, and features of glioma tissues and the expression of *PSMA3-AS1* were studied via the χ^2 test. In three independent experiments, data were expressed as mean ± SD. Besides, the Student's t test and one-way ANOVA were adopted for assessment of intergroup or intragroup differences, respectively. $P<0.05$ represented a difference that was statistically significant.

Results

Characteristics and expression of *PSMA3-AS1* in glioma

Through analyzing the GSE103227 microarray, *PSMA3-AS1* was found to be highly expressed in glioma. Differentially expressed lncRNAs were identified according to the criteria of $P<0.05$ and fold change > 2. The differently expressed lncRNAs including *PSMA3-AS1* with most significance was identified in glioma. To ascertain these results, *PSMA3-AS1* expression was assessed in 20 pairs of glioma tissues and adjacent normal tissues via qRT-PCR. In comparison with paired adjacent tissues, *PSMA3-AS1* exhibited a notably raised expression in glioma tissues (Figure 1A). The PSMA3-AS1 was elevated in patients with advanced stages of gliomas (III + IV vs I + II, $P<0.05$). Detailed information is presented in Table 1. Identically, NHA cells had a lower *PSMA3-AS1* expression than human glioma cells (Figure 1B). Notably, LN229 and U251 had high expressions compared with the other glioma cell lines, so the two cell lines were chosen for the loss-of-function assays. We performed the nuclear and cytoplasmic separation experiment and found that PSMA3-AS1 mainly located in the cytoplasm (Figure 1C). This result revealed that PSMA3-AS1 will mainly take part in the post-transcriptional regulation of genes related to glioma.

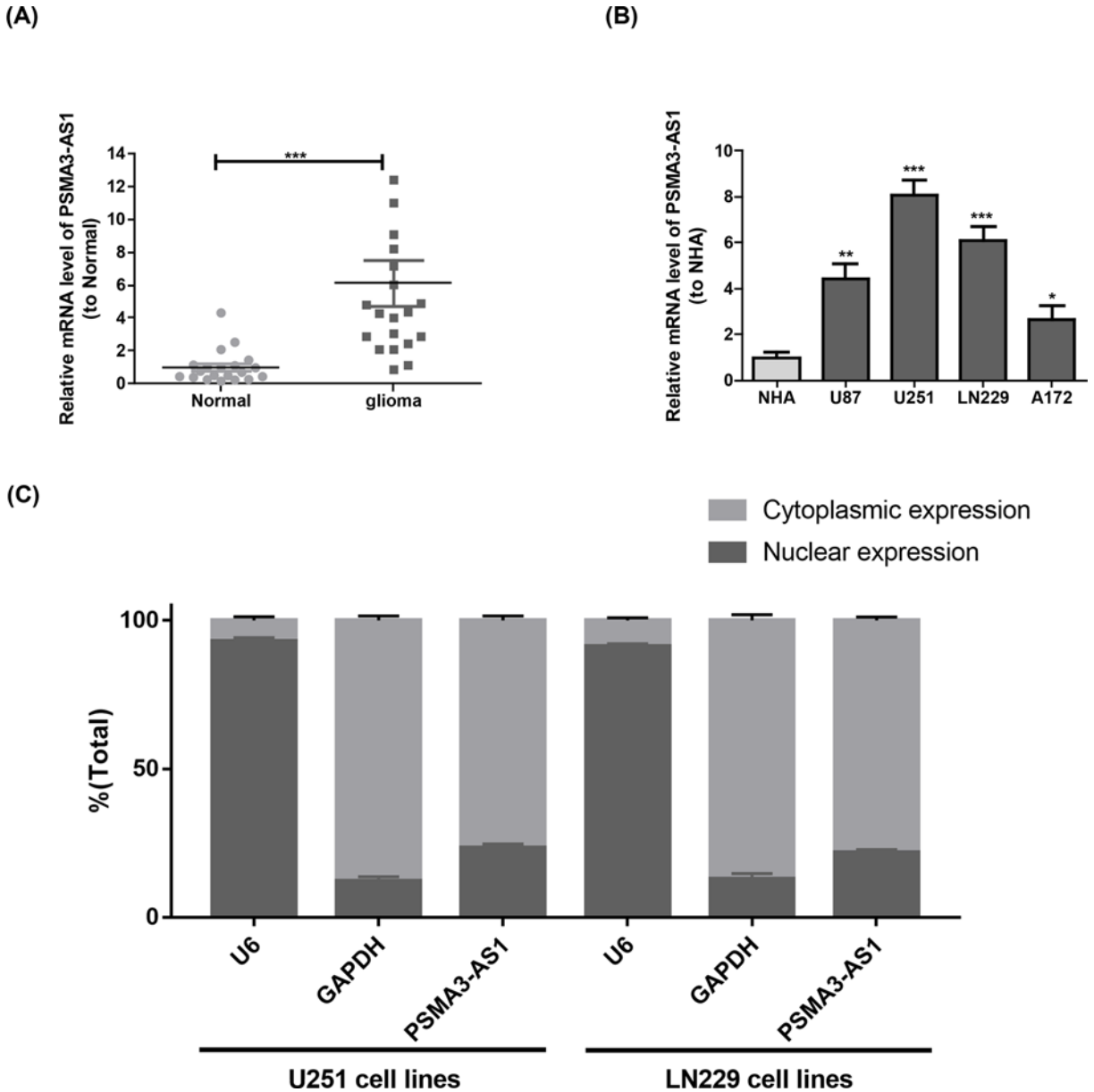

Figure 1. Relative *PSMA3-AS1* expressions in glioma tissues and cell lines

(**A**) The relative expressions of *PSMA3-AS1* in glioma tissues and adjacent normal tissues (n=20) detected via qRT-PCR. (**B**) Relative *PSMA3-AS1* expressions in one normal cell line and glioma cell lines. (**C**) Nuclear and cytoplasmic separation experiment of U251 and LN299. Three independent experiments are conducted. Error bars represent mean ± SD of at least three experiments. *P<0.05; **P<0.01; ***P<0.001.

PSMA3-AS1 down-regulation impeded the migration, proliferation and invasion of glioma cells

Since *PSMA3-AS1* in glioma cell lines was raised, whose biological function was further unfolded *in vitro*. LN229 and U251 were transfected with si-*PSMA3-AS1-1*, si-*PSMA3-AS1-2* or si-*PSMA3-AS13*, respectively. It was found in qRT-PCR that *PSMA3-AS1* expressions in LN229 and U251 were reduced after transfection, among which the sharpest decrease in *PSMA3-AS1* expression was caused by si-*PSMA3-AS1-2* transfection (Figure 2A). According to CCK-8 assay, the growth of LN229 and U251 was remarkably blocked by si-*PSMA3-AS1-2* transfection instead of si-NC transfection (Figure 2B). Subsequently, EdU-positive cells were confirmed to be down-regulated in LN229 and U251 by EdU assay (Figure 2C). The results of the plate clone experiment were consistent with those of the previous

Bioscience Reports (2020) **40** BSR20191571
https://doi.org/10.1042/BSR20191571

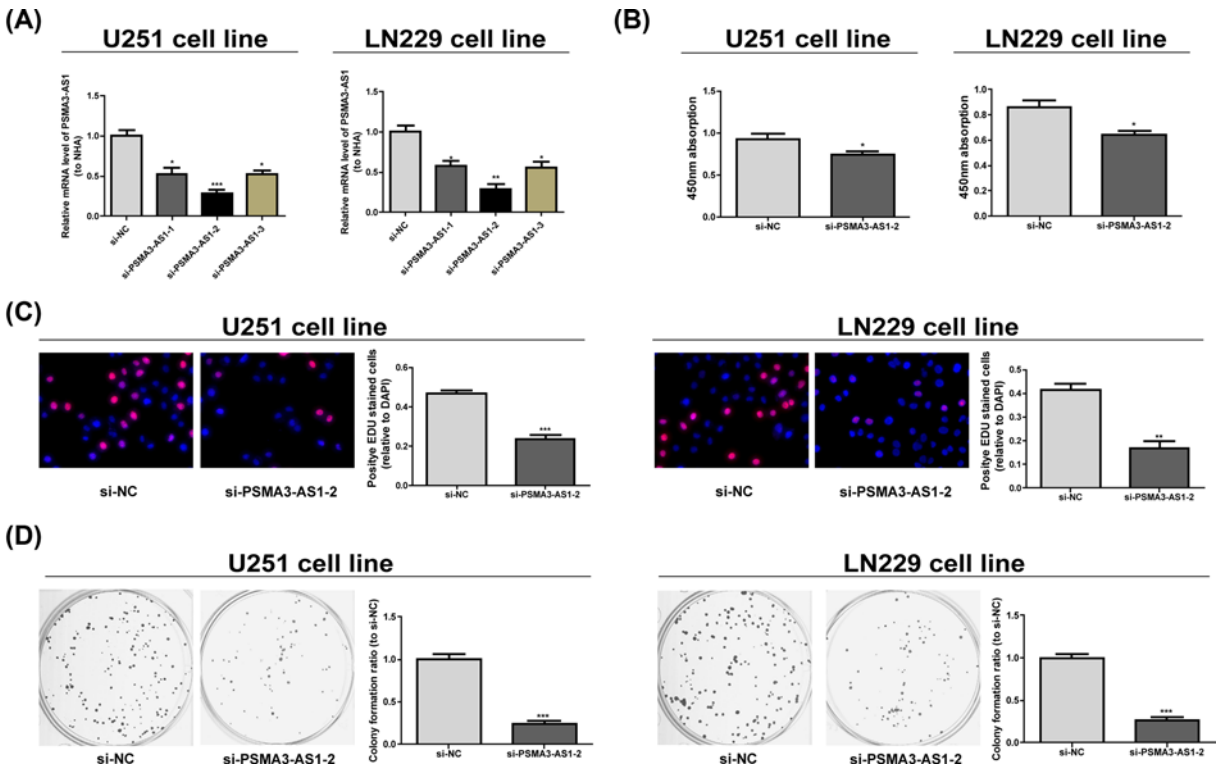

Figure 2. Regulation of *PSMA3-AS1* on the growth and proliferation of LN229 and U251

(**A**) Assessment of the expressions of *PSMA3-AS1* in LN229 and U251 treated with different si-*PSMA3-AS1* sequences by qRT-PCR. (**B**) Measurement of cell viabilities of LN229 and U251 that are stably transfected with si-NC or si-*PSMA3-AS1-2*, respectively by CCK-8 assay. (**C**) Verification of the functions of *PSMA3-AS1* in the proliferation of LN229 and U251 by EdU assays. EdU-positive cells are counted and recorded. (**D**) Verification of the functions of *PSMA3-AS1* in the proliferation of LN229 and U251 via clone assay. Three independent experiments are conducted. Error bars represent mean ± SD of at least three experiments. $^{*}P<0.05$; $^{**}P<0.01$; $^{***}P<0.001$.

experiments, and the colony formation of glioma cells after si-*PSMA3-AS1-2* transfection was significantly inhibited (Figure 2D).

Functions of *PSMA3-AS1* in cell migration and invasion were then examined via Transwell assay. It was found that knockdown of *PSMA3-AS1* decreased the number of migrated cells in LN229 and U251 (Figure 3A). Similarly, *PSMA3-AS1* down-regulation suppressed the invasion of LN229 and U251 (Figure 3B). As epithelial–mesenchymal transition (EMT) exerts a pivotal effect on glioma cell invasion and migration, the role of *PSMA3-AS1* in epithelial characteristics was further investigated. The expressions of ZO-1 (an epithelial marker), Vimentin (a mesenchymal marker) and Snail1 and Twist (EMT-related transcription factors) were measured. As shown in Figure 3C, si-*PSMA3-AS1-2* promoted ZO-1 at the mRNA and protein levels, while inhibiting Vimentin, Snail1 and Twist. It can be seen that reduction in *PSMA3-AS1* evidently suppresses the migration, proliferation and invasion of glioma cells.

MiR-302a-3p adjusted the proliferation, migration and invasion of glioma cells by targeting *PSMA3-AS1*'s 3′UTR

There has been more and more evidence that lncRNAs are able to adjust miRNAs' effects by sponging them. StarBase revealed that miR-302a-3p and 3′UTR of *PSMA3-AS1* were complementary as they shared binding sites (Figure 4A), which was then validated *via* the dual luciferase reporter assay. According to the results, it was not the luciferase activity of *PSMA3-AS1* MUT but that of *PSMA3-AS1* WT that was markedly weakened by miR-302a-3p (Figure 4B). The miR-302a-3p mRNA level was decreased in glioma tissues and was negatively correlated with PSMA3-AS1(Figure 4C,D). At the same time, the content of miR-302a-3p in glioma cell lines was measured by qRT-PCR, which was lower than that of NHA (Figure 4E). Furthermore, miR-302a-3p in LN229 and U251 exhibited a higher expression in

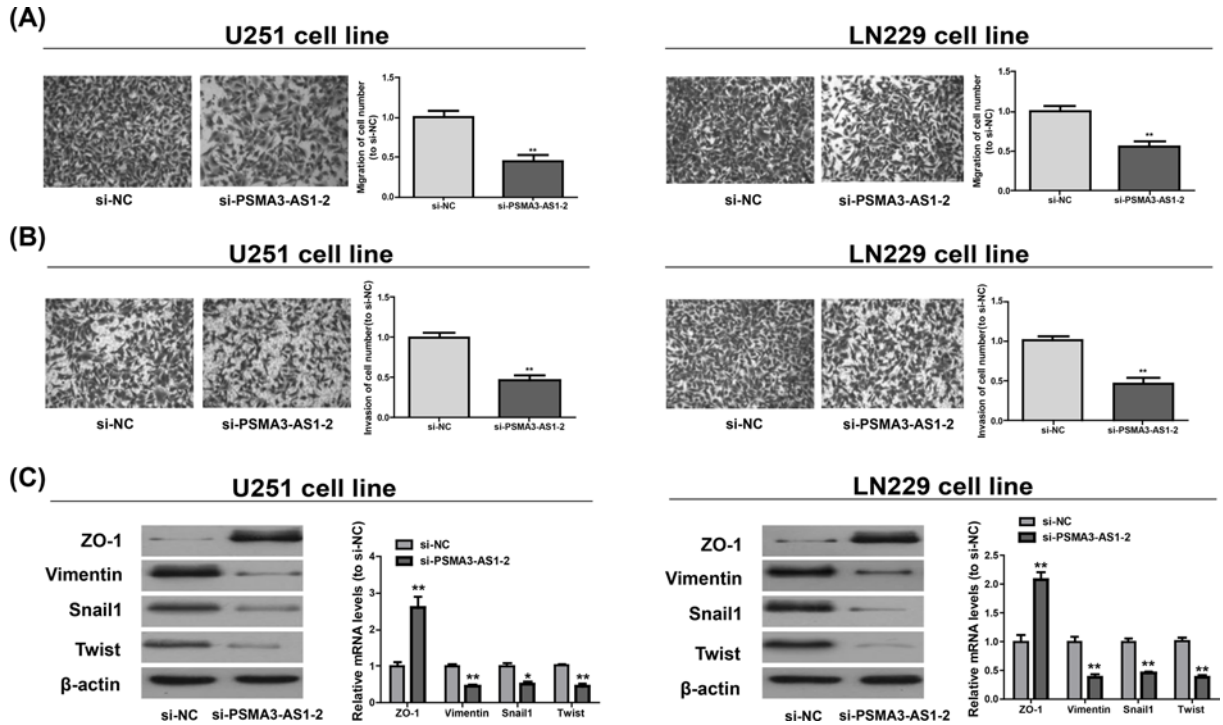

Figure 3. Regulation of *PSMA3-AS1* on the migration and invasion of LN229 and U251

(**A**,**B**) The percentage of cell suffering from migration and invasion number in LN229 and U251 after si-*PSMA3-AS1-2* transfection is detected. (**C**) The protein and mRNA levels of ZO-1, Vimentin, Snail1 and Twist in LN229 and U251 upon down-expression of *PSMA3-AS1*. Three independent experiments are conducted. Error bars represent mean ± SD of at least triplicate experiments. $^{*}P<0.05$; $^{**}P<0.01$.

PSMA3-AS1 knockdown group than si-NC group (Figure 4F). Subsequently, the roles of *PSMA3-AS1*/miR-302a-3p in the migration, proliferation and invasion of glioma cells were continued to be discussed. It could be discovered that miR-302a-3p overexpression prominently blocked cell proliferation (Figure 4G) and decreased the cells suffering from metastasis and invasion (Figure 4H), and *PSMA3-AS1* knockdown in U251 cells could enhance these effects.

MiR-302a-3p targets *RAB22A*

Bioinformatics analysis was carried out and revealed that miR-302a-3p and 3′UTR of *RAB22A* mRNA were complementary as they shared binding sites (Figure 5A). Luciferase reporter assay ascertained that there was a molecular binding within *RAB22A* and miR-302a-3p (Figure 5B). qRT-PCR (Figure 5C) manifested that *RAB22A* in glioma cells was markedly higher than that in NHA. The TargetScan and miRDB were used to predict the target gene of miR-302a-3p, and CROT, EDNRB, LATS2, OXR1, ZNF367, RAB22A and NR2C2 were selected. Then the U251 and LN229 cell lines were transfected to detected these genes. Only RAB22A was decreased by miR-302a-3p(Figure 5D,E), and the other genes did not change after miR-302a-3p mimics transfection. Meanwhile, the decreased miR-302a-3p could rescue the inhibition effect of si-RAB22A on RAB22A protein expression(Figure 5F). Meanwhile, the decreased cell proliferation, migration and invasion induced by si-RAB22A were recovered by miR-302a-3p inhibitor(Figure 5G,H). Briefly, it can be concluded that miR-302a-3p targets RAB22A, and *RAB22A* expression may be adjusted by *PSMA3-AS1* in a positive manner via sponging miR-302a-3p, evidencing the role of the *PSMA3-AS1*/miR-302a-3p/*RAB22A* pathway.

PSMA3-AS1 partially negatively adjusted miR-302a-3p *in vivo* to cause tumor formation

Findings *in vitro* were then ascertained by the establishment of a nude mouse model of xenograft. Substantial differences were observed in tumor formation in the sh-NC, sh-*PSMA3-AS1* or sh-*PSMA3-AS1*+miR-302a-3p inhibitor groups (Figure 6A). Additionally, it was demonstrated in the time-dependent analysis that sh-*PSMA3-AS1* group

Bioscience Reports (2020) **40** BSR20191571
https://doi.org/10.1042/BSR20191571

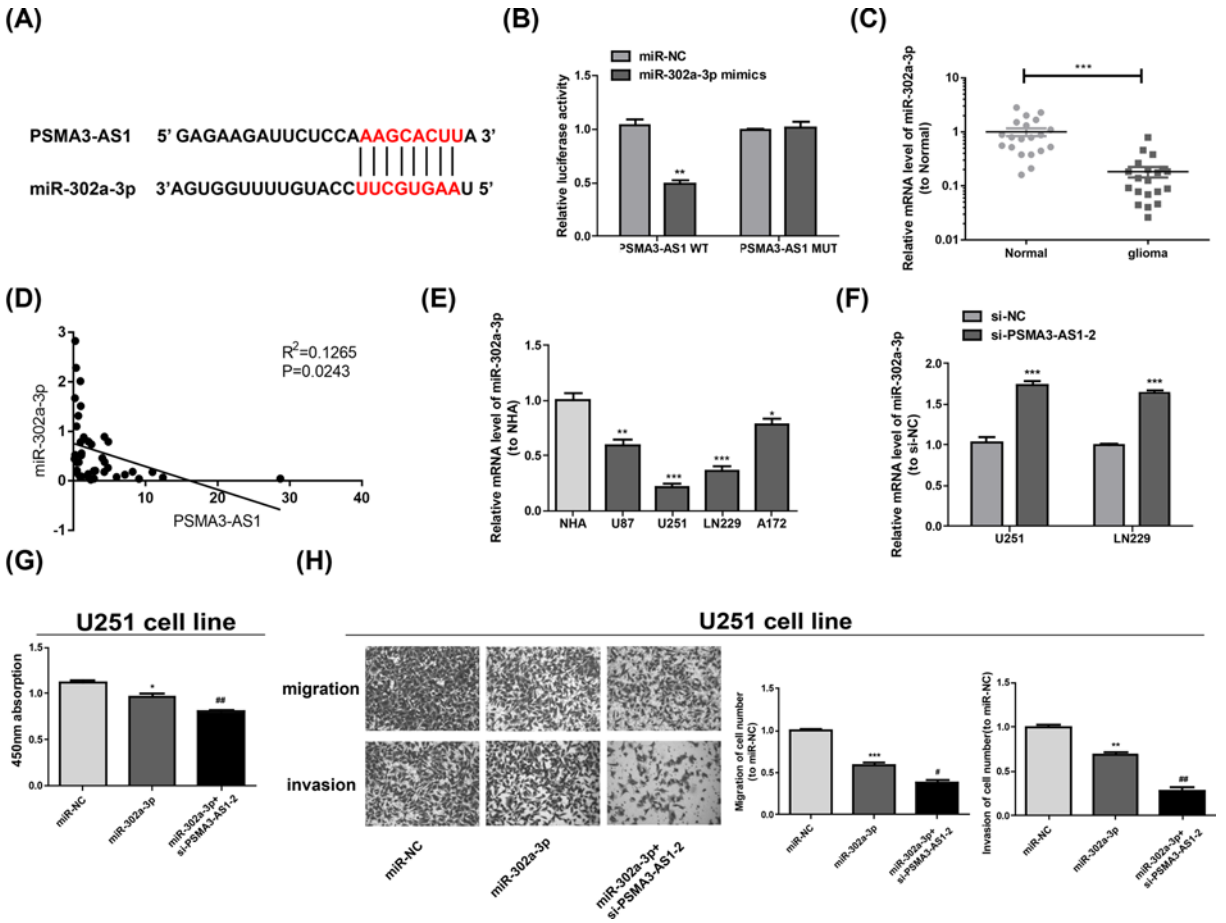

Figure 4. MiR-302a-3p is a direct target of *PSMA3-AS1*

(**A**) The target miRNA regulated by *PSMA3-AS1* is predicted using StarBase. Binding sites between miR-302a-3p and *PSMA3-AS1* are shown. (**B**) 293T cells are co-transfected with the luciferase reporter constructs containing *PSMA3-AS1* WT or *PSMA3-AS1* MUT sequences and miR-302a-3p or miR-NC, and then the relative luciferase activity is examined. $^{**}P<0.01$ vs. miR-NC. (**C**) Relative miR-302a-3p expression in normal and glioma tissues. (**D**) The correlation of miR-302a-3p and PSMA3-AS1 of glioma tissues ($P=0.0243$). (**E**) Relative miR-302a-3p expression in a normal cell line NHA and glioma cell lines. $^{*}P<0.05$; $^{**}P<0.01$; $^{***}P<0.001$ vs. NHA. (**F**) LN229 and U251 are transfected with si-NC or si-*PSMA3-AS1-2*. 48 h later, miR-302a-3p expression is measured via qRT-PCR. $^{***}P<0.001$ vs. si-NC. (**G**,**H**) The proliferation is determined via CCK-8 assay and migration and invasion via Transwell assay in U251 transfected with miR-NC, miR-302a-3p or miR-302a-3p+si-*PSMA3-AS1-2*. Three independent experiments are carried out. Error bars represent mean ± SD of at least three experiments. $^{*}P<0.05$; $^{**}P<0.01$; $^{***}P<0.001$ vs. miR-NC; $^{\#}P<0.05$; $^{\#\#}P<0.01$ vs. miR-302a-3p.

had smaller tumor volumes than sh-NC group, and sh-*PSMA3-AS1*+miR-302a-3p inhibitor could rescue the effect of sh-PSMA3-AS1 as a tumor suppressor. (Figure 6B). Identically, tumor weight in all groups had the same results as the tumor volume (Figure 6C). MiR-302a-3p (Figure 6D) and *RAB22A* (Figure 6E,F) expressions in xenografts were monitored via qRT-PCR and Western blot, the results of which illustrated that *PSMA3-AS1* knockdown evidently lowered the expression level of *RAB22A* but elevated that of miR-302a-3p, which was rescued by simultaneous miR-302a-3p inhibition, in consistent with findings *in vitro*.

Discussion

In recent years, an enormous body of research has revealed that lncRNAs are not inhibited in malignant tumors and become targets for diagnosing and treating cancers, including glioma [17–19]. However, there is almost no research related to *PSMA3-AS1*. Interestingly, it was found in this study that *PSMA3-AS1* might be associated with glioma by microarray analysis, which was then further verified and studied in population and cells. Moreover, *PSMA3-AS1*

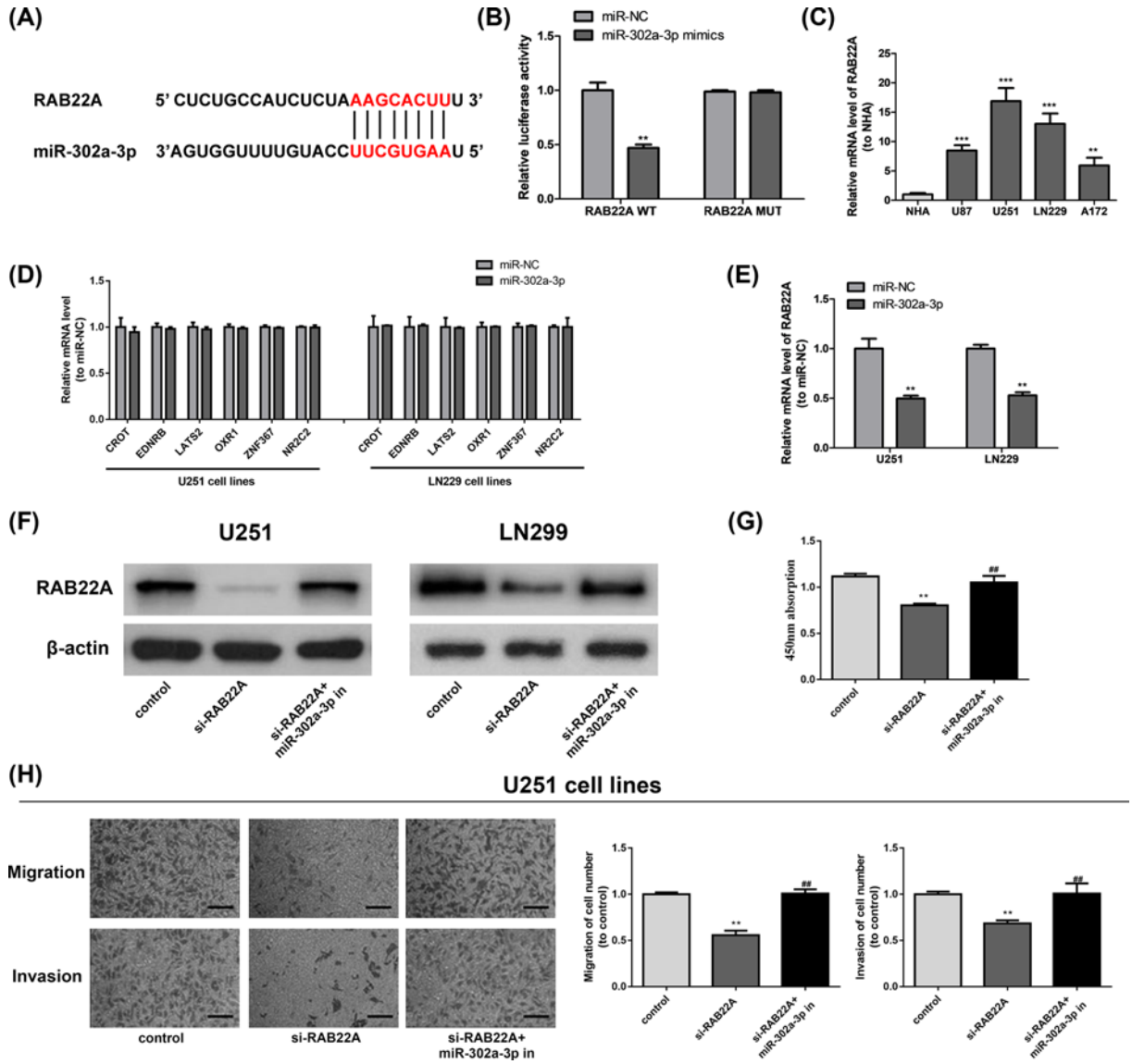

Figure 5. *PSMA3-AS1* positively regulates *RAB22A* expression via miR-302a-3p

(**A**) Predication of interaction between miR-302a-3p and *RAB22A* via bioinformatics analysis. (**B**) Luciferase vitality in the combination within miR-302a-3p/miR-NC and *RAB22A* WT/MUT shown in luciferase reporter assay. ***$P<0.001$ vs. miR-NC. (**C**) Relative *RAB22A* expression in a normal cell line NHA and glioma cell lines. **$P<0.01$; ***$P<0.001$ vs. NHA. (**D**,**E**) Expression of predicted miR-302a-3p target genes (*CROT, EDNRB, LATS2, OXR1, ZNF367, RAB22A* and *NR2C2*) in U251 and LN229 cell lines transfected by miR-302a-3p. (**F**) *RAB22A* expressions in LN229 and U251 detected by Western blotting. (**G**,**H**) The proliferation is determined via CCK-8 assay and migration and invasion via Transwell assay in U251 transfected with control, si-RAB22A or si-RAN22A+miR-302a-3p inhibitor. Three independent experiments are conducted. Error bars represent mean ± SD of at least three experiments. **$P<0.01$vs. miR-NC.$^{\#}P<0.05$; $^{\#\#}P<0.01$ vs. si-RAB22A.

was discovered to be remarkably raised in glioma samples and cells, and the reduced *PSMA3-AS1* greatly inhibited glioma cell proliferation, migration and invasion, which was verified by assays *in vitro* and *in vivo*. These results suggest that PSMA3-AS1 might be a new idea for glioma treatment.

There is a close correlation between lncRNAs biological function and miRNAs and their interactions substantially adjust the progression of numerous cancers [20–22]. In this research, *PSMA3-AS1* was ascertained to directly bind to miR-302a-3p and reduce the expression of the latter in glioma cells. Identical to the results of *PSMA3-AS1*

Bioscience Reports (2020) **40** BSR20191571
https://doi.org/10.1042/BSR20191571

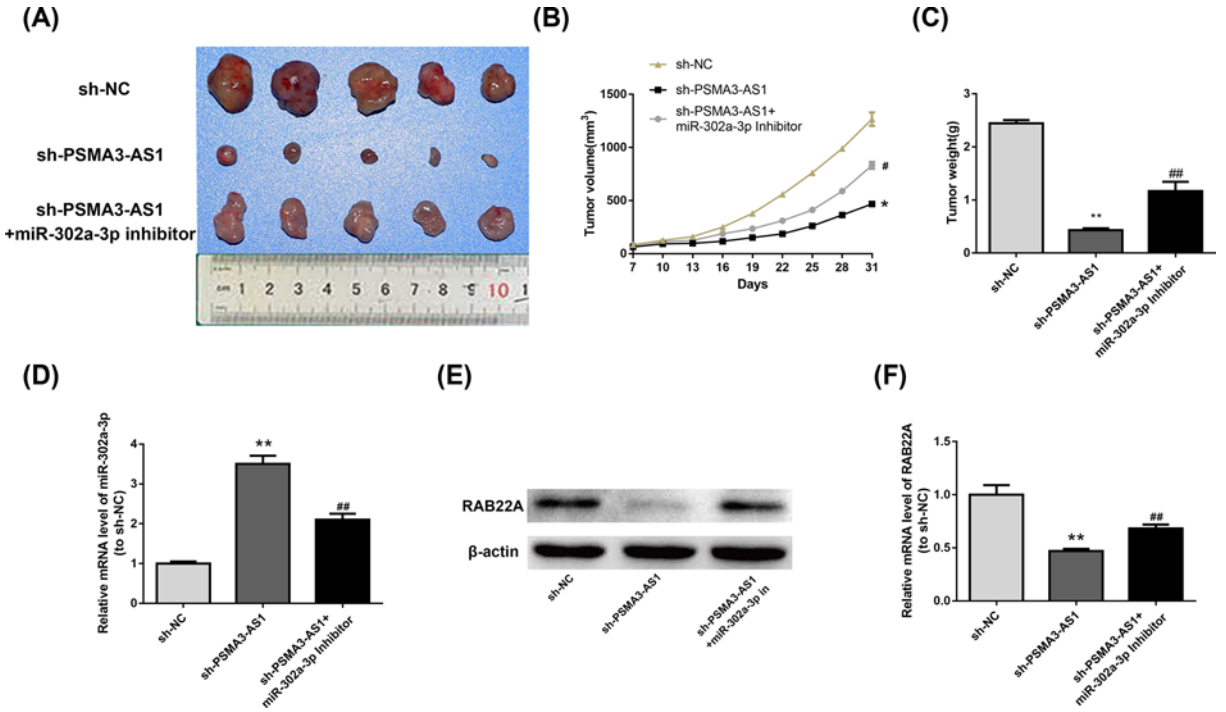

Figure 6. *PSMA3-AS1* oncogenic activity is in part through negative regulation of miR-302a-3p *in vivo*

(**A**) Distinctive images of tumor formation of xenograft in nude mice from sh-NC, sh-*PSMA3-AS1* or sh-*PSMA3-AS1*+miR-302a-3p inhibitor groups, respectively (n=3 in each group). (**B**) Tumor volume of mice measured in every 3 days in sh-NC, sh-*PSMA3-AS1* or sh-*PSMA3-AS1*+miR-302a-3p inhibitor groups, respectively. (**C**) Changes in the tumor weight in nude mice from sh-NC, sh-*PSMA3-AS1* or sh-*PSMA3-AS1*+miR-302a-3p inhibitor groups, respectively (n=3 in each group). (**D**) Determination of miR-302a-3p expression in xenografts via qRT-PCR. (**E**,**F**) The protein and mRNA levels of *RAB22A* in xenografts. Three independent experiments are carried out. Error bars represent mean ± SD of at least three experiments. $^{*}P<0.05$; $^{**}P<0.01$ vs. sh-NC; $^{\#}P<0.05$; $^{\#\#}P<0.01$ vs. sh-*PSMA3-AS1*.

knockdown, the migration, proliferation and invasion of glioma cells were notably impeded by miR-302a-3p overexpression, but the function of *PSMA3-AS1* knockdown in the glioma cell behaviors was remarkably stimulated by it. Actually, miR-302a-3p suppresses multiple tumors, such as hepatoblastoma [16] and gastric cancer [23], so it was hypothesized that *PSMA3-AS1*, a host gene of snoRNAs, targets miR-302a-3p to accelerate glioma progression.

It has been found that *RAB22A*, a member of RAS oncogene family, is markedly raised in numerous human cancers [24]. In recent years, epigenetical mechanism has been discovered to adjust *RAB22A* expression in human cancers, and multiple miRNAs directly target *RAB22A* to inhibit tumors [25–27]. Moreover, Yin Y et al. demonstrated that miR-204-5p decreases *RAB22A* so as to strengthen the chemotherapeutic sensitivity [28]. Similarly, it was found that *RAB22A* was up-regulated in glioma. Moreover, *RAB22A* was regarded as miR-302a-3p's target in glioma examined by bioinformatics analysis. *In vivo* assays were carried out, which further ascertained that *PSMA3-AS1* knockdown was capable of down-regulating *RAB22A* expression by raising miR-302a-3p, thus slowing down glioma progression.

To sum up, the results of assays *in vitro* and *in vivo* unfold that *PSMA3-AS1* functions as an oncogene to accelerate glioma progression. The findings indicate that tumor formation and the growth, migration and invasion of glioma cells are impeded by *PSMA3-AS1* knockdown. The present study first reveals the underlying mechanism that *PSMA3-AS1* influences the cell proliferation, migration and invasion via miR-302a-3p/*RAB22A* pathway in the tumorigenesis of glioma, providing new ideas for glioma treatment.

Competing Interests

The authors declare that there are no competing interests associated with the manuscript.

Funding

The authors declare that there are no sources of funding to be acknowledged.

Author Contribution

Mei-fen Sun made substantial contributions to conception and design. Li-li Zhou made acquisition of data, performed the experiments. Li-li Zhou, Meng Zhang and Yan-zhen Zhang wrote the draft manuscript. All authors contributed to the reviewing of the manuscript, and approved the final manuscript for submission.

Ethics Approval

The research was approved by the Ethics Committee of Heze No. 3 People's Hospital (Shandong, China). All population-related study was carried out in accordance with the World Medical Association Declaration of Helsinki, and that all subjects written informed consent.

Abbreviations

CCK-8, Cell Counting Kit-8; CNS, central nervous system; EdU, 5-Ethynyl-2′-deoxyuridine; EMT, epithelial–mesenchymal transition; GAPDH, glyceraldehyde-3-phosphate dehydrogenase; lncRNA, long non-coding RNA; MUT, mutant; qRT-PCR, quantitative real-time PCR; siRNA, small interfering RNA; WT, wildtype; 3′UTR, 3′-untranslated region; PSMA3-AS1, PSMA3 antisense RNA 1; qPCR, Quantitative Polymerase Chain Reaction; RAB22A, ras-related protein Rab-22A; ZO-1, zonula occludens-1.

References

1 Leng, Y., Wang, X., Liao, W. and Cao, Y. (2018) Radiomics in gliomas: a promising assistance for glioma clinical research. *Zhong Nan Da Xue Xue Bao Yi Xue Ban* **43**, 354–359
2 Sturm, D., Pfister, S.M. and Jones, D.T.W. (2017) Pediatric gliomas: current concepts on diagnosis, biology, and clinical management. *J. Clin. Oncol.* **35**, 2370–2377, https://doi.org/10.1200/JCO.2017.73.0242
3 Saxena, S. and Jha, S. (2017) Role of NOD-like receptors in glioma angiogenesis: insights into future therapeutic interventions. *Cytokine Growth Factor Rev.* **34**, 15–26, https://doi.org/10.1016/j.cytogfr.2017.02.001
4 Bell, C., Dowson, N., Puttick, S., Gal, Y., Thomas, P., Fay, M. et al. (2015) Increasing feasibility and utility of (18)F-FDOPA PET for the management of glioma. *Nucl. Med. Biol.* **42**, 788–795, https://doi.org/10.1016/j.nucmedbio.2015.06.001
5 Schwarzer, A., Emmrich, S., Schmidt, F., Beck, D., Ng, M., Reimer, C. et al. (2017) The non-coding RNA landscape of human hematopoiesis and leukemia. *Nat. Commun.* **8**, 218, https://doi.org/10.1038/s41467-017-00212-4
6 Li, H., Zhu, H., Zhou, Y., Wang, H., Niu, Z., Shen, Y. et al. (2017) Long non-coding RNA MSTO2P promotes the proliferation and colony formation in gastric cancer by indirectly regulating miR-335 expression. *Tumour Biol.* **39**, 1010428317705506
7 Zhu, Q., Lv, T., Wu, Y., Shi, X., Liu, H. and Song, Y. (2017) Long non-coding RNA 00312 regulated by HOXA5 inhibits tumour proliferation and promotes apoptosis in non-small cell lung cancer. *J. Cell. Mol. Med.* **21**, 2184–2198, https://doi.org/10.1111/jcmm.13142
8 Weidle, U.H., Birzele, F., Kollmorgen, G. and Ruger, R. (2017) Long non-coding RNAs and their role in metastasis. *Cancer Genomics Proteomics* **14**, 143–160, https://doi.org/10.21873/cgp.20027
9 Xia, L., Nie, D., Wang, G., Sun, C. and Chen, G. (2019) FER1L4/miR-372/E2F1 works as a ceRNA system to regulate the proliferation and cell cycle of glioma cells. *J. Cell. Mol. Med.* **23**, 3224–3233, https://doi.org/10.1111/jcmm.14198
10 Ni, W., Xia, Y., Bi, Y., Wen, F., Hu, D. and Luo, L. (2019) FoxD2-AS1 promotes glioma progression by regulating miR-185-5P/HMGA2 axis and PI3K/AKT signaling pathway. *Aging (Albany N.Y.)* **11**, 1427–1439
11 Yang, C., Wang, L., Sun, J., Zhou, J.H., Tan, Y.L., Wang, Y.F. et al. (2019) Identification of long noncoding RNA HERC2P2 as a tumor suppressor in glioma. *Carcinogenesis* **40**, 956–964, https://doi.org/10.1093/carcin/bgz043
12 Pan, X., Li, D., Huo, J., Kong, F., Yang, H. and Ma, X. (2018) LINC01016 promotes the malignant phenotype of endometrial cancer cells by regulating the miR-302a-3p/miR-3130-3p/NFYA/SATB1 axis. *Cell Death Dis.* **9**, 303, https://doi.org/10.1038/s41419-018-0291-9
13 Guo, H., Ingolia, N.T., Weissman, J.S. and Bartel, D.P. (2010) Mammalian microRNAs predominantly act to decrease target mRNA levels. *Nature* **466**, 835–840, https://doi.org/10.1038/nature09267
14 Tuo, Y.L., Li, X.M. and Luo, J. (2015) Long noncoding RNA UCA1 modulates breast cancer cell growth and apoptosis through decreasing tumor suppressive miR-143. *Eur. Rev. Med. Pharmacol. Sci.* **19**, 3403–3411
15 Zhang, Z., Li, J., Guo, H., Wang, F., Ma, L., Du, C. et al. (2019) BRM transcriptionally regulates miR-302a-3p to target SOCS5/STAT3 signaling axis to potentiate pancreatic cancer metastasis. *Cancer Lett.* **449**, 215–225, https://doi.org/10.1016/j.canlet.2019.02.031
16 Ye, Y., Song, Y., Zhuang, J., Wang, G., Ni, J., Zhang, S. et al. (2018) MicroRNA-302a-3p suppresses hepatocellular carcinoma progression by inhibiting proliferation and invasion. *Onco Targets Ther.* **11**, 8175–8184, https://doi.org/10.2147/OTT.S167162
17 Cui, B., Li, B., Liu, Q. and Cui, Y. (2017) lncRNA CCAT1 promotes glioma tumorigenesis by sponging miR-181b. *J. Cell. Biochem.* **118**, 4548–4557, https://doi.org/10.1002/jcb.26116
18 Shi, J., Dong, B., Cao, J., Mao, Y., Guan, W., Peng, Y. et al. (2017) Long non-coding RNA in glioma: signaling pathways. *Oncotarget* **8**, 27582–27592, https://doi.org/10.18632/oncotarget.15175
19 Zhao, W., Sun, C. and Cui, Z. (2017) A long noncoding RNA UCA1 promotes proliferation and predicts poor prognosis in glioma. *Clin. Transl. Oncol.* **19**, 735–741, https://doi.org/10.1007/s12094-016-1597-7
20 Ballantyne, M.D., McDonald, R.A. and Baker, A.H. (2016) lncRNA/MicroRNA interactions in the vasculature. *Clin. Pharmacol. Ther.* **99**, 494–501, https://doi.org/10.1002/cpt.355

21 Wieczorek, E. and Reszka, E. (2018) mRNA, microRNA and lncRNA as novel bladder tumor markers. *Clin. Chim. Acta* **477**, 141–153, https://doi.org/10.1016/j.cca.2017.12.009

22 Cao, M.X., Jiang, Y.P., Tang, Y.L. and Liang, X.H. (2017) The crosstalk between lncRNA and microRNA in cancer metastasis: orchestrating the epithelial-mesenchymal plasticity. *Oncotarget* **8**, 12472–12483, https://doi.org/10.18632/oncotarget.13957

23 Yang, C. and Deng, S.P. (2019) Mechanism of hsa-miR-302a-3p-targeted VEGFA in the inhibition of proliferation of gastric cancer cell. *Sichuan Da Xue Xue Bao Yi Xue Ban* **50**, 13–19

24 Su, F., Chen, Y., Zhu, S., Li, F., Zhao, S., Wu, L. et al. (2016) RAB22A overexpression promotes the tumor growth of melanoma. *Oncotarget* **7**, 71744–71753, https://doi.org/10.18632/oncotarget.12329

25 Zheng, S., Jiang, F., Ge, D., Tang, J., Chen, H., Yang, J. et al. (2019) LncRNA SNHG3/miRNA-151a-3p/RAB22A axis regulates invasion and migration of osteosarcoma. *Biomed. Pharmacother.* **112**, 108695, https://doi.org/10.1016/j.biopha.2019.108695

26 Sun, L., He, M., Xu, N., Xu, D.H., Ben-David, Y., Yang, Z.Y. et al. (2018) Regulation of RAB22A by mir-193b inhibits breast cancer growth and metastasis mediated by exosomes. *Int. J. Oncol.* **53**, 2705–2714

27 Bian, Z., Jin, L., Zhang, J., Yin, Y., Quan, C., Hu, Y. et al. (2016) LncRNA-UCA1 enhances cell proliferation and 5-fluorouracil resistance in colorectal cancer by inhibiting miR-204-5p. *Sci. Rep.* **6**, 23892, https://doi.org/10.1038/srep23892

28 Yin, Y., Zhang, B., Wang, W., Fei, B., Quan, C., Zhang, J. et al. (2014) miR-204-5p inhibits proliferation and invasion and enhances chemotherapeutic sensitivity of colorectal cancer cells by downregulating RAB22A. *Clin. Cancer Res.* **20**, 6187–6199, https://doi.org/10.1158/1078-0432.CCR-14-1030